Analysis of the IEEE 802.11 DCF for Wireless Seismic Data Acquisition Networks

Aliyu Makama, Koojana Kuladinithi, Andreas Timm-Giel
Institute of communication Networks, Hamburg University of Technology, Germany
{aliyu.makama, koojana.kuladinithi, timm-giel}@tuhh.de

2022 32nd International Telecommunication Networks and Applications Conference (ITNAC) | 978-1-6654-7103-9/22/$31.00 ©2022 IEEE | DOI: 10.1109/ITNAC55475.2022.9998354

***Abstract*—Owing to the nature of traffic and architecture of Wireless Seismic Data Acquisition (WSDA) networks also referred to as Wireless Geophone Networks (WGN), we propose a model that analytically investigates the performance of IEEE 802.11 protocol for single-hop ad hoc WGNs under unsaturated traffic and non-ideal channel conditions. Although several IEEE 802.11 models have been presented in literature, some inaccuracies exist with respect to modeling IEEE 802.11-based WGNs. Our model focuses primarily on singling out the inaccuracies in modeling the backoff procedure and packet drop probability as some of the deviance with the existing literature. Expressions for MAC delay, throughput, collision probability, and average duration a node spends during the backoff procedure before decrementing its counter were proposed. Furthermore, the model investigates an optimal number of geophones that could be supported within a subnetwork based on the proposed WGN architecture in [16]. The model was evaluated analytically in MATLAB and validated using simulation in OMNeT++ discrete event simulator.**

***Index Terms*—Seismic survey, Wireless Seismic Data Acquisition (WSDA), Wireless Geophone Network (WGN), Central Control Unit (CCU), Distributed Coordination Function (DCF);**

I. INTRODUCTION

Seismic survey is a method of obtaining an image of the earth's sub-surface structure in order to determine optimal places to drill for oil and gas. In onshore seismic survey, an energy source generates variable frequency waves (shots) that propagate through the earth's surface. These waves are reflected and refracted as they hit various subsurface layers and are recorded at the surface by devices called geophones for a duration of time referred to as listening or recording period. The reflected signals are then amplified, digitized, multiplexed and sent down to the central control unit (CCU) for further processing to come up with a graphical representation of the earth's subsurface. Conventional cable-based seismic survey methods are known to have drawbacks such as complications in survey logistics, deployment costs, unwieldy flexibility in survey planning, as well as survey downtime. These drawbacks brought about the need for oil and gas industries to move from cable-based to wireless telemetry systems. This involves geophones equipped with wireless transceivers to form a network of wireless geophones. WGNs often employ a large-scale deployment of geophones (10's of thousands with future surveys targeting 100's of thousands) in the survey area according to the orthogonal geometry [1].

Unlike traditional wireless sensor networks (WSNs), WGNs come with a number of challenges such as high data rate requirement due to large aggregate seismic data volume, large scale geophone deployment, low latency, wireless coverage and connectivity etc. Regard for imposed cost, communication coverage, high bit rate, and power consumption are some of the key factors to consider when selecting wireless technology for WGNs. However, obtaining a single technology that addresses all these issues can be quite difficult. A viable starting point for investigating this scenario is to use off-the-shelf IEEE 802.11 based technologies like 802.11 g/n, 802.11ah, and 802.11af as they provide high data rate and long communication range. Consequently, analysis of how geophones access the shared wireless medium based on the IEEE 802.11 Distributed Coordination Function (DCF) [2] is of essential importance. Due to the nature of WGN specific traffic pattern, our model considers unsaturated traffic condition as geophones can be in a situation where they have no packet in their buffer. More substantive, analysis of the MAC delay will prove effective in terms of estimating the geophone data transfer duration within a single seismic shot.

IEEE 802.11 defines a medium access control (MAC) sublayer which controls how nodes access the radio frequency (RF) channel via logical functions which includes DCF, the optional Point Coordination Function (PCF) and Hybrid Coordination Function (HCF) [2]. DCF is the fundamental channel access mechanism in IEEE 802.11 protocol that provides contention based service. It is based on the carrier sense multiple access with collision avoidance (CSMA/CA) algorithm where collisions are managed according to the exponential backoff algorithm. There are two access mechanisms employed in DCF, the Request-To-Send/Clear-To-Send (RTS/CTS) and the basic access method. In this work, the basic access mechanism was considered. An error can occur as a result of collisions due to concurrent packet transmission by nodes, or due to wireless channel errors.

The contributions in this paper are three folded: First we proposed a model that investigates the general behavior of a single-hop IEEE 802.11 DCF based on WGNs specific network attributes in terms of traffic pattern and architecture in [16]. This will serve as a general tool for faster performance investigation of IEEE 802.11-based WGNs as compared to simulation. Secondly, an analysis and modeling of the wireless channel behavior when a reference geophone enters backoff procedure was presented. This is to estimate the average

2022 32nd International Telecommunication Networks and Applications Conference (ITNAC)

duration a node spends before decrementing its counter during the backoff procedure. Finally, we present an expression for the probability that a packet transmission fails, as well as for the throughput and MAC delay which can be applied to estimate the WGN network performance and also perform scalability and parameter investigation. The rest of the paper is organized as follows: Section II gives a general review on the related work. Section III explains the WGN traffic generation pattern. In section IV, the Markov chain model for a single geophone station under the IEEE 802.11 protocol as well as the channel state Markov model were presented. Section V presents the WGNs performance evaluation in terms of throughput, delay, collision probability, as well as model validation using OMNeT++ discrete event simulator. Finally, section VI gives the conclusion and future work.

II. RELATED WORK

Bianchi in [3] was the first to model the IEEE 802.11 DCF, based on the CSMA/CA protocol with a two dimensional Markov chain describing the binary exponential back-off mechanism. However, some realistic assumptions, and attributes as defined in the standard like i.e. freezing of the back-off counter when the channels is sensed busy, and retransmission limits are lacking in the model. Many improvements to the Bianchi model in terms of a more generalized and practical network settings have been presented in literature.

For improvements with the assumption of saturated traffic conditions, authors in [4] presented an analytical expression to compute the system capacity, packet drop probabilities, and mean frame delays in an error-prone radio channel. In [5], an analytical model to compute the saturation throughput and delay for different frame aggregation techniques in the IEEE 802.11n under error-prone channel conditions is presented. They compared the analytical model with simulation using the uni-directional and bi-directional methods of transferring data of the A-MSDU and A-MPDU frame aggregation schemes.

In [6], authors presented a performance analysis of the IEEE 802.11ac under hidden nodes and saturated traffic conditions. They investigated the effect of using different primary channels and bandwidth as the new features in IEEE 802.11ac DCF. The assumption of saturated traffic condition is however unrealistic in most 802.11 networks as in majority of real situations with considerable idle periods. As such, various articles proposed a model extension of [3] that takes into account unsaturated traffic condition. Different approaches were employed in the literature to model the unsaturated traffic behavior of a station.

An approach to extend the discrete-time Markov chain model in [3] is given in [7], [8], [15]. Their models incorporate an additional state to account for the situation where a node has an empty buffer. Another approach in [9], [10] involves applying queuing theory analysis to estimate probability that the stations buffer is empty, which means that the station will not compete for the medium access. However, in all the above literature, the probability to drop a packet after "m" number of retries was not considered in their models.

Some literature focus on extending [3] to properly estimate the time duration spent by a node during the backoff procedure. The authors in [11], [12] take into account the effect of back-off counter freezing in their models i.e. the busy medium condition during the back-off procedure. However, they did not consider the circumstance where the packet is been dropped after the maximum retransmission limit is reached. Authors in [18] considered the packet drop probability in their model in addition to back-off counter freezing, but however failed to incorporate an additional state to account for the situation where a station has an empty queue, and also assumed ideal channel conditions. Authors in [13], [14] included the maximum retransmission limit and packet drop in their models and did not consider the back-off counter freezing situation during the back-off procedure. Authors in [7] incorporate network coding to analyze the performance of the 802.11 DCF protocol while addressing the packet drop and back-off counter freezing probabilities.

Nonetheless, to properly analyze an IEEE 802.11-based geophone station under the proposed WGN traffic model described in section III, the model has to take into account unsaturated traffic conditions, real channel conditions, back-off counter decrementing probability, as well as probability to drop a packet. Therefore, in this paper we focus on combining and extending the models presented in [3], [15], [18] to incorporate features of the IEEE 802.11 DCF in accordance with the WGN application scenario and the standard such as packet drop after certain transmission retries, counter freezing and decrementing probability during backoff procedure, unsaturated traffic conditions.

III. WIRELESS GEOPHONE NETWORK TRAFFIC MODEL

Most seismic data acquisition applications require data to be transmitted or downloaded after the geophone recording period T_{rp}. In this model however, data is transmitted during T_{rp}, referred to as Recording Period Data Acquisition (RPDA). This allows for real-time seismic data transfer, which in turn may increase the overall productivity of the survey. Seismic data samples s_n collected by geophones for a given period of time T_{ds} during T_{rp} for a particular sweep, are transmitted to the CCU at the end of every T_{ds} period prior to the next T_{ds}, until the end of T_{rp}, as depicted in Fig. 1. T_{ds} represents the seismic data sample accumulation time and defines how frequent packets are sent by geophones in the network. In this work, a typical value of $T_{rp} = 5\,\mathrm{s}$ is used. Generally, the traffic model is a non-saturated periodic traffic with deterministic packet arrival rate. While the data generated per geophone is rather small ($48\,\mathrm{kbit/s}$), i.e., assuming an Analog-to-Digital Converter (ADC) resolution of $24\,\mathrm{bit}$, with signal sampled at $0.5\,\mathrm{ms}$ interval, the aggregate data generated within a subnetwork is significantly large. For a single-hop subnetwork with up to 200 geophones maximum, a network capacity of about $9.6\,\mathrm{Mbit/s}$ will be required [17]. In this work, a T_{ds} value of $0.25\,\mathrm{s}$ is defined. This means that each geophone will acquire 500 seismic data samples (s_n) each of size $3\,\mathrm{B}$ over the period of $0.25\,\mathrm{s}$. These data samples will

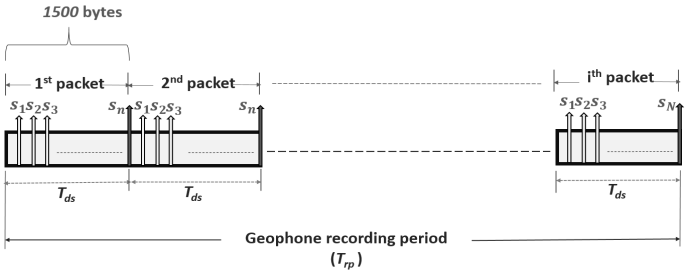

Fig. 1: Geophone recording period data acquisition traffic pattern

be placed in a packet of fixed size $1500\,\mathrm{B}$ at the application layer and sent over the wireless medium prior to the next T_{ds} until the end of a geophone recording period T_{rp} of $5\,\mathrm{s}$. As such, it will be appropriate to model the geophone buffer as a $D/M/1$ queue due to the deterministic packet inter-arrival time ($1/\lambda = 0.25\,\mathrm{s}$), and a stochastic departure process resulting from the random nature of the underlying CSMA/CA protocol in the MAC layer. Due to the significantly large inter-arrival time of packets ($0.25\,\mathrm{s}$), we assume a binary queue length.

IV. NETWORK MODEL

This section presents the basic pretext under which the Markov model for a geophone node was proposed and used to analyze the overall system throughput. In addition, the condition of the wireless channel during backoff procedure from a reference geophone point of view is modeled using a Markov chain. This is beneficial when computing medium access delay, especially the amount of time spent by a geophone during backoff procedure before successfully transmitting a packet, as well as the total delay experienced by a packet. All considerations in the models are in accordance with WSDA and the traffic model discussed in Section III.

A. Geophone Markov Chain Model

To model the 802.11 DCF geophone station behavior under the geophone recording period acquisition technique, we combine the model considerations in [3], [15], [18]. The contribution in our model compared to previous work are shown in Fig. 2 by the thick highlighted components.

1) Model Assumptions and Notations: Based on the following postulations, a Bi-Dimensional Markov model is established as depicted in Fig. 2: (i) Fixed number of homogeneous geophone nodes with no hidden terminals, and fixed packet size under unsaturated traffic and real channel conditions in accordance with the proposed traffic model in [16]. (ii) The geophone node has at least one packet in its buffer with probability "q", and an empty buffer with the probability $1-q$. (iii) A packet transmission from a geophone fails either due to collision with probability P_c, which is independent of the previous number of retransmission suffered, or due to channel error with the probability P_{ce}. (iv) A geophone transmits a packet in any randomly chosen time slot with stationary probability τ. Considering the deterministic inter-arrival time of packets as discussed in Section III, "q" is approximated as expressed in (1).

$$q = \lambda / E[s] \tag{1}$$

λ represents the packet arrival rate, and $E[s]$ is the mean service rate computed as sum of the time to successfully transmit a packet T_s, collision time T_c, and mean backoff duration over the average number or retransmission.

A successful transmission of a packet occurs only if no channel errors and no packet collision occurs. This event happens with a probability:

$$P_s = (1 - P_c)(1 - P_{ce}) \tag{2}$$

The packet transmission then fails with a probability

$$P_f = 1 - P_s = P_c + P_{ce} - P_c P_{ce} \tag{3}$$

Even though the mathematical modeling of the DCF holds for any family of the IEEE 802.11 standard, the network parameters of IEEE 802.11g/n were selected as reference. A geophone can either be in state S_E or $S_{i,j}$ ($\forall:\ 0 \le i \le m,\ 0 \le j \le W_i - 1$). The state S_E represents the situation in which a geophone node has no packet in its buffer for transmission. i and j in state $S_{i,j}$ represents the transmission stage and backoff counter value of a geophone respectively. For every unsuccessful packet transmission, i is incremented and the backoff counter value is doubled until it reaches a maximum value $i = m$, beyond which the packet is dropped. W_i represents the contention window value at the i^{th} transmission stage chosen randomly between $[0, W_i - 1]$ and is defined as:

$$W_i = \begin{cases} W_0 = CW_{min} & i = 0 \\ 2^i(CW_{min} + 1) - 1 & 0 < i < m' - 1 \\ CW_{max} & m' \le i \le m \end{cases} \tag{4}$$

where m denotes the maximum transmission stage, W_0 represents the minimum contention window (CW_{min}) value at the initial transmission attempt, CW_{max} is the maximum contention window value, and $m' = \log_2\big((CW_{max} + 1)/(CW_{min} + 1)\big)$. The value of W_i doubles for each $i + 1$ transmission stage, and has a value CW_{max} at $i = m$. The packet is dropped if it encounters $m+1$ transmission attempts and W_i resets to CW_{min} value. A geophone remains in state S_E with the probability $1 - q$. Upon arrival of a frame with probability q at the buffer, the geophone exits state S_E to the initial transmission stage and senses the channel. If the channel is sensed idle for a DIFS duration, the geophone then transmits directly at state $S_{(0,0)}$. If the channel is sensed busy, the geophone enters backoff and randomly selects a backoff counter value from $[0, W_0 - 1]$ with the probability $1/W_0$. The geophone backoff counter duration is expressed in terms of slot time (σ) and W_i as $backoff = \mathrm{rand}[0, W_i] \times \sigma$, where the function "$rand$" defines the random selection of the counter value uniformly distributed in the range $[0, W_i]$.

During the backoff procedure, the backoff counter value decrements with the probability P_{cd} when the geophone senses the channel idle and freezes with the probability

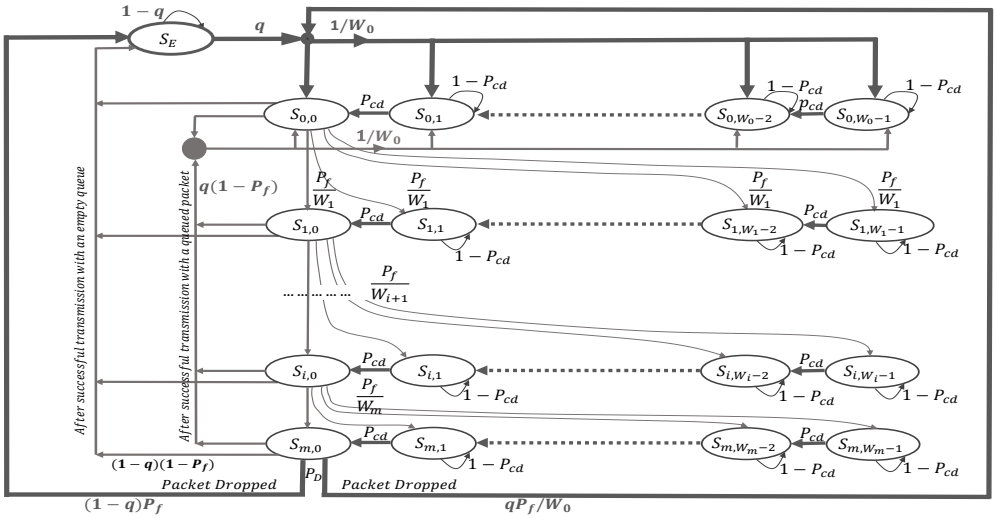

Fig. 2: Markov model for a single geophone station

$1 - P_{cd}$ when the channel is sensed busy. The node attempts transmission only when the backoff counter value reaches zero at state $S_{(i,0)}$. However, if the transmission attempt fails due to collision or due to channel errors, the geophone moves to the $i+1$ transmission stage and draws a new backoff counter value with the probability P_f/W_{i+1} where P_f is the probability that the packet transmission fails. If the packet is successfully transmitted at any of the transmission stages $S_{(i,0)}$ and the geophone has another packet queued at its buffer, the geophone then moves to state $S_{(0,j)}$ with probability $q(1-P_f)/W_0$. If the geophone draws a contention window value of zero after a successful transmission at state $S_{(0,j)}$, it can then directly access the channel and transmit again. If however, the geophone has an empty buffer immediately after a successful transmission, it moves to state S_E with the probability $(1-q)(1-P_f)$ and awaits the arrival of a new frame. Furthermore, if the packet transmission fails at state $S_{(m,0)}$, the packet is dropped with the probability $P_D = P_f^{m+1}$ and the geophone moves to either state S_E or state $S_{0,j}$ with the probabilities $(1-q)P_f$ and qP_f/W_0 respectively. The Markov chain model in Fig. 2 incorporates the following transition probabilities:

$$\begin{cases} P\{S_{i,j-1}|S_{i,j}\} = P_{cd} & \\ P\{S_{i,j}|S_{i,j}\} = 1 - P_{cd} & \\ P\{S_{i+1,j}|S_{i,0}\} = P_f/W_{i+1} & 1 \le i \le m \\ P\{S_{0,j}|S_{i,0}\} = \dfrac{q(1-P_f)}{W_0} & 1 \le j \le W_0 \\ P\{S_E|S_{i,0}\} = (1-q)(1-P_f) & 0 \le i < m \\ P\{S_{0,j}|S_E\} = q/W_0 & j \in (0, W_0 - 1) \\ P\{S_E|S_E\} = 1 - q & \\ P\{S_{0,j}|S_{m,0}\} = q(P_f/W_0) & j \in (0, W_0 - 1) \\ P\{S_E|S_{m,0}\} = (1-q)P_f & \end{cases} \tag{5}$$

2) Stationary Probability: Let τ be the stationary probability that a geophone transmits a packet in a randomly chosen time slot. To determine the stationary distribution of the Markov chain in Fig. 2, let $\gamma_{i,j}$ represent the probability that in any given time slot, a geophone occupies a given state $S_{i,j}$, and γ_{S_E} the probability of being in state S_E

$$\gamma_{i,j} = \lim_{t\to\infty} P\Big[s(t) = i, \gamma(t) = j\Big] \;\forall\; i \in [0, m], \forall\; j \in [0, W_i - 1] \tag{6}$$

γ_{S_E} accounts for the fact that after a successful transmission at any of the state $S_{i,0}$, state S_E can be reached with probability $(1-q)(1-P_f)$.

$$\gamma_{S_E} = (1-q)(1-P_f)\sum_{i=0}^{m}\gamma_{(i,0)} + (1-q)\gamma_{S_E} + (1-q)P_f\gamma_{m,0} \tag{7}$$

Equation (8) gives the expression for the normalization conditions, which yields the solution for $\gamma_{0,0}$ in (10) [7].

$$\sum_{i=0}^{m}\sum_{j=0}^{W_{i-1}}\gamma_{(i,j)} + \gamma_{S_E} = 1 \tag{8}$$

A detailed expansion for (8) is given in [3] and [15]. Therefore, the stationary probability τ that a geophone transmits a packet in a randomly chosen time slot is expressed in (9), which can the be further expressed as in (11) [15].

$$\tau = \sum_{i=0}^{m}\gamma_{(i,0)} = \gamma_{0,0}\frac{1-P_f^{m+1}}{1-P_f} \tag{9}$$

$$\gamma_{0,0} = \frac{2qP_{cd}(1-P_f)(1-2P_f)}{q\Big[W(1-P_f)(1-(2P_f)^{m+1}) + (1-2P_f)(2P_{cd}-1)(1-(P_f)^{m+1})\Big] + 2(1-q)P_{cd}(1-P_f)(1-2P_f)} \tag{10}$$

$$\tau = \frac{2qP_{cd}(1-2P_f)(1-P_f^{m+1})}{q\Big[W(1-P_f)(1-(2P_f)^{m+1}) + (1-2P_f)(2P_{cd}-1)(1-(P_f)^{m+1})\Big] + 2(1-q)P_{cd}(1-P_f)(1-2P_f)} \tag{11}$$

For N geophone nodes, a packet transmitted from the reference geophone experience collision with the probability $P_c = 1 - (1-\tau)^{N-1}$ if at least any one of the remaining $N-1$ geophones is simultaneously transmitting.

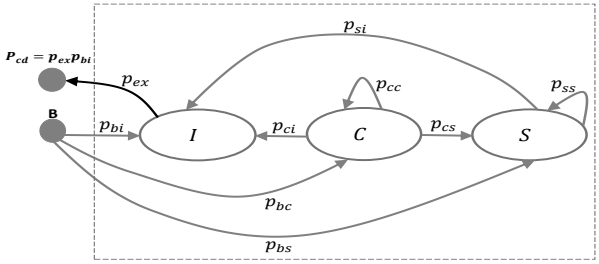

Fig. 3: Channel state Markov model for a single geophone station

The packet is lost either due to channel errors or collision with the probability

$$P_f = P_c + P_{ce} - P_c P_{ce} \tag{12}$$

The probability that the reference geophone transmits its packet successfully is the probability that exactly one geophone transmits on the channel, as given in (13).

$$P_{T_{xG}} = N\tau(1-\tau)^{N-1} \tag{13}$$

The backoff counter decrements with the probability P_{cd} when the channel is sensed idle i.e., when all remaining geophones are not transmitting as expressed in (14), and freezes with probability $1 - P_{cd}$.

$$P_{cd} = (1-\tau)^{N-1} \tag{14}$$

B. The Channel State Markov Chain Model

To properly model the time spend by a geophone during a backoff procedure before decrementing its counter value, it is important to take a closer look at the state of the channel when the reference node is in backoff. Fig. 3 shows the Markov chain model of the channel during the backoff procedure. The model is an extension of the model presented in [18] to take into consideration the seismic data acquisition traffic model presented in Section 2. The states I, C, and S represents the state of the channel being idle, having a failed transmission attempt due collision or channel errors, and successful transmission respectively. B represents the point at which the reference geophone enters backoff process. p_{bi} is the probability that the reference geophone enters backoff and encounters the channel in the idle state I. From the reference geophone point of view, when all of the remaining geophones are not transmitting, the channel is considered idle.

$$p_{bi} = (1-\tau)^{N-1} \tag{15}$$

The reference node then decrements its counter with the probability P_{cd}. The probability p_{ex} is always equals to 1. Similarly, p_{bc} is the probability that the reference geophone enters backoff and encounters the channel in state C. This can be as a result of a failed packet transmission either due to packet collisions when two or more geophones transmit simultaneously during a slot time, or due to channel errors. Such event occurs when the channel is neither idle nor having any ongoing successful transmission. In compliance with the protocol, when an erroneous frame transmission occurs, the node in question has to defer the channel access for an Extended Inter frame Space (EIFS) duration. The EIFS begins at the end of the erroneous frame transmission when the channel is declared idle by the Physical layer. $EIFS = DIFS + SIFS + T_{xACK}$, where T_{xACK} is the time taken to send an acknowledgment frame at the PHY mandatory rate. The channel remains in state C with probability p_{cc} and exits with probability p_{ci} to state I or with probability p_{cs} to state S. p_{ci} can be defined as the probability that none of the geophones with failed transmission selects zero as their new backoff counter after a collision process. If "c" is the number of geophones with failed transmission, then the probability that none of the geophones with failed transmission have zero as a current backoff counter value is $(1-(1/CW_{avg}))^c$ where CW_{avg} is the average contention window size over all transmission stages.

$$CW_{avg} = \frac{1-P_f}{1-P_D}\sum_{i=0}^{m} P_f^i W_i \tag{16}$$

Then the probability that no geophone with failed transmission selects zero as a new backoff counter value is expressed as:

$$p_{ci} = \sum_{c=2}^{N-1}\Big(1-\frac{1}{CW_{avg}}\Big)^c \tag{17}$$

The transition from state C to S occurs only if one geophone selects zero as a new backoff counter value after failed transmission attempt with the probability p_{cs}.

$$p_{cs} = \sum_{c=2}^{N-1} c\Big(\frac{1}{CW_{avg}}\Big)\Big(1-\frac{1}{CW_{avg}}\Big)^{c-1} \tag{18}$$

Note that only a geophone that is successfully transmitting a packet has full access to the channel, and the channel remains at the successful transmission state if that geophone selects a backoff counter value of zero in the next time slot. As such, the transition from state S to C is not possible. p_{bs} is the probability that the reference node enters backoff and finds the channel busy as a result of a successful packet transmission. The channel remains in this state with the probability p_{ss} if the geophone that successfully transmits its packet chooses a backoff counter value of zero when transmitting its next packet, and exits with probability p_{si} to state I otherwise. Equation (19) gives a summary of the transition probabilities [18]:

$$\begin{cases} P\{I|B\} = p_{bi} = (1-\tau)^{N-1} \\ P\{S|B\} = p_{bs} = \binom{N-1}{1}\tau(1-\tau)^{N-2} \\ P\{C|B\} = p_{bc} = 1 - p_{bi} - p_{bs} \\ P\{S|S\} = p_{ss} = 1/w_0 \\ P\{I|S\} = p_{si} = 1 - p_{ss} \\ P\{C|C\} = p_{cc} = 1 - p_{ci} - p_{cs} \\ P\{I|C\} = p_{ci} = \sum_{c=2}^{N-1}\Big(1-\frac{1}{CW_{avg}}\Big)^c \\ P\{S|C\} = p_{cs} = \sum_{c=2}^{N-1} c\Big(\frac{1}{CW_{avg}}\Big)\Big(1-\frac{1}{CW_{avg}}\Big)^{c-1} \\ P\{C|S\} = p_{sc} = 0 \end{cases} \tag{19}$$

Let $\eth$ be the average time taken by a geophone before decrementing its counter during a backoff procedure. To compute

$\eth$, we first look at the duration a reference geophone spends at a given backoff process when the state of the channel is idle (σ_I), having successful transmission (σ_S) or collision (σ_C). For σ_I, the reference geophone awaits one time slot before decrementing its counter (i.e., $\sigma_I = 1$). Similarly, when the channel is found busy by the reference geophone that enters backoff, it has to wait for a duration of the successful transmission of packet (T_s) and any other subsequent successful transmission. As such, σ_S can be expressed as given in (20).

$$\sigma_S = \frac{1}{1-p_{ss}} T_s + \frac{p_{si}}{1-p_{ss}} \sigma_I \tag{20}$$

If the reference node encounters the channel busy as a result of failed packet transmission, it waits for the collision or packet error duration (T_c) plus other successive failed or successful transmission. σ_C can then be expressed as given in (21).

$$\sigma_C = \Big(\sum_{i=1}^{m} i p_{cc}^{i} \Big) T_c + \frac{p_{cs}}{1-p_{cc}} \sigma_S + \frac{p_{ci}}{1-p_{cc}} \sigma_I \tag{21}$$

T_s and T_c represents the average time the channel is sensed busy due to a successful transmission and during a failed packet transmission respectively. Equation (22) gives the expression for T_s and T_c for basic access mechanism.

$$\begin{cases} T_s^{bas} = DIFS + T_H + T_{E[P]} + SIFS + 2\delta + T_{ACK} \\ T_c^{bas} = DIFS + T_H + T_{E[P]} + \delta \end{cases} \tag{22}$$

Furthermore, the reference geophone can enter the backoff process either from a prior backoff state or from a transmission state. Therefore, these two cases should be taken into consideration when computing the average slot duration during the backoff procedure.

- If the node enters from a prior backoff state, the average slot duration ($\eth_B$) can be expressed as in (23).

$$\eth_B = \frac{1}{p_{cd}} \Big[p_{bi}\sigma_I + p_{bs}\sigma_S + p_{bc}\sigma_C \Big] \tag{23}$$

- If the node enters backoff procedure from a transmission state, the average slot duration ($\eth_T$) can be expressed as in (24).

$$\eth_T = q\Big(\frac{(CW_{avg}-1)}{CW_{avg}} \Big) \Big[p_{bi}\sigma_I + p_{bs}\sigma_S + p_{bc}\sigma_C \Big] \tag{24}$$

In view of the fact that a geophone enters the backoff state from a previous backoff state with the probability $1-\tau$, and enters from a transmission state with the probability τ, the average slot duration a reference geophone waits before decrementing its counter during the backoff procedure can then be expressed as in (25).

$$\eth = (1-\tau)\eth_B + \tau \eth_T \tag{25}$$

V. PERFORMANCE EVALUATION

A. System Throughput

Throughput is defined as the amount of data packets successfully transferred over the channel within a particular slot time as given in (26), where L_P is the packet length including headers transmitted over the channel in bit and σ_D is the duration of a slot time.

$$S_T = L_P / \sigma_D \tag{26}$$

The normalized system throughput can be computed as given in (27) [3]:

$$S_T = \frac{P_{suc} P_{T_x} (1-P_{ce}) L_P}{\begin{array}{c}(1-P_{T_x})\sigma + P_{suc}P_{T_x}(1-P_{ce})T_s \\ +(1-P_{suc})P_{T_x}T_c + P_{suc}P_{T_x}P_{ce}T_e\end{array}} \tag{27}$$

where σ is the slot time, P_{ce} is the frame error probability due to channel conditions, P_{T_x} is the probability that there is at least one transmission in a the considered time slot given by:

$$P_{T_x} = 1 - (1-\tau)^N \tag{28}$$

and P_{suc} is the probability that a packet transmission ongoing on the channel is successful. This is equivalent to the probability that exactly one geophone transmits ($P_{T_{xG}}$) conditioned over the probability that at least one geophone transmits (P_{T_x}).

$$P_{suc} = \frac{P_{T_{xG}}}{P_{T_x}} = \frac{N\tau(1-\tau)^{N-1}}{1-(1-\tau)^N} \tag{29}$$

T_e represents the frame slot duration due to channel errors given by;

$$T_e = T_H + T_{L[P]} + T_{ACK} \tag{30}$$

B. Offered Load (η)

The theoretical offered load (η) for different network sizes can be computed using the relation expressed in (31).

$$\eta = (L_P \times N \times N_{ps})/(T_{rx}) \quad \text{bit/s} \tag{31}$$

where N is the number of geophones in the network, N_{ps} is the number of packets sent per geophone over the duration T_{rp}, and T_{rx} is the time taken to receive all data packets at the destination node.

C. Medium Access Delay (D_{MAC})

We define D_{MAC} as the delay experienced by a frame from the instant it arrives at MAC layer till its successful transmission to the intended receiver. Consider the case where a geophone successfully transmits a packet at the initial transmission attempt (i.e., $i = 0$), the MAC delay can then be expressed as:

$$D_{MAC(0)} = T_s + ((W_0 - 1)/2)\eth \tag{32}$$

Similarly, for all consecutive successful transmissions at stage i, D_{MAC} can be expressed as in (33), where $\overline{W_j}$ is the average backoff counter value at any given transmission stage $j \in i$ expressed as $(W_j - 1)/2$.

$$D_{MAC(i)} = T_s + iT_c + \sum_{j=0}^{i} \overline{W_j}\eth \qquad 0 < i \leq m \tag{33}$$

Constraining (33) over the probability P_{suc} that the packet is successfully transmitted in any of the transmission stages i, as

well as packet drop probability P_D, the medium access delay can generally be expressed as:

$$D_{MAC} = \frac{1}{1-P_D} \sum_{i=0}^{m} P_{suc}^{(i)} \Big[T_s + iT_c + \sum_{j=0}^{i} \overline{W_j}\tilde{\sigma} \Big] \qquad (34)$$

D. Model Validation

A comparison between analytical and simulation results is presented. The simulation was carried out for 10 runs and results were evaluated with 95% confidence level. Table I shows the network parameters used for both analytical and simulation evaluation. The parameters are in accordance with orthogonal frequency division multiplexing (OFDM) based WLANs with traffic in the Best Effort or Background Access Categories, employed in the IEEE 802.11a/g/n standards. OMNeT++ discrete event simulator [19], which has an implementation of the IEEE 802.11 DCF was used to validate the model. Typical network parameters for the IEEE 802.11g/n were employed in both simulation and analytical evaluations.

TABLE I: Analytical and Simulation Parameters

Parameter	Value
Packet Payload	1500 B
MAC & PHY Header	224 bit, 192 bit
ACK	112 bit+PHY Header
CW_{min}, CW_{max}	32, 1024
Bit rate	12 & 54 Mbit/s
Packet retransmission limit	6
Propagation delay	1 µs
SIFS, slotTime, DIFS	10 µs, 20 µs, 50 µs
Simulation time	20 s

1) Scenario Configuration: Fig. 4 illustrates the scenario under which the performance evaluation was carried out. The network consists of four receiver lines positioned $200\,\mathrm{m}$ apart, each having geophones placed at an interval of $25\,\mathrm{m}$ along the line. Geophones transmit their data to the sink node in single-hop, operating in ad hoc mode. Traffic is generated according to the model described in Section 2. With the fixed payload size of $1500\,\mathrm{B}$, each geophone will generate a packet every $250\,\mathrm{ms}$, and 20 packets over the $5\,\mathrm{s}$ recording period duration.

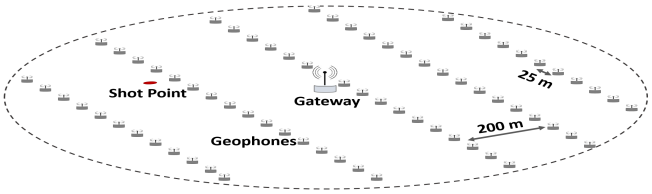

Fig. 4: WGN scenario: IEEE 802.11 ad hoc mode

Fig. 5a shows the offered load to the network along with the analytical and simulated throughput behavior as a function of number of geophones for different data rates (12 and 54 $\mathrm{Mbit/s}$). The offered load is computed analytically using (31). The simulated throughput closely matches the analytical results for both data rates. However, with $12\mathrm{Mbit/s}$ data rate, it can be noticed that the throughput begins to drop when the number of geophones in the network reaches a certain value (176). This is because higher number of nodes results in increased network traffic. Thus, the offered load approaches the maximum capacity the network can handle (e.g. $8.9\,\mathrm{Mbit/s}$ for 176 nodes), thereby resulting in congestion and subsequently increased number of collisions. Moreover, due to additional protocol headers (UDP, IP, MAC, and PHY), the offered data rate increases even further. This consequently leads to an exponential increase in packet retransmissions (computed from simulation as the ratio of number of packets re-transmitted to the number of packets successfully received) as can be seen in Fig. 5b. Thus, some packets are dropped due to the fact that maximum retransmission limit has been exceeded. This effect is also captured in the analytical estimation where the throughput begins to gradually drop at this value. Thus, our model assumption of geophone unsaturated traffic condition and binary queue size only holds if the injected traffic is considerably less than the network capacity especially for lower data rates. Furthermore, we compared our model to the Felemban non-saturated model presented in [18] as shown in Fig. 5a. Our model deviates from theirs by approximately 10% for $12\mathrm{Mbit/s}$ data rate, starting from network size of 40 where the traffic load approaches the network capacity, and deviates even further with increased retransmissions. This is because the state S_E was not consider in their model, but rather extend their saturated model to account for the unsaturated case by iteratively calculating the probability that a node has no packet to transmit in its buffer, assuming Poisson packet arrivals.

Fig. 5c shows the analytical and simulated MAC delay for 12 and 54 $\mathrm{Mbit/s}$ data rates. The delay is computed analytically from (34) for each packet generated by a geophone, averaged over all nodes in the network. It includes the delay added due to backoff and retransmissions suffered by each packet. As expected, the MAC delay decreases with increase in data rate. The analytical results follows the simulation for both data rates until the network has no significant collisions. The analytical result slightly deviates from the simulation with higher number of collisions. This is because with more geophones in the network, probability P_f (computed as a function of P_c and P_{ce} in the model) increases and deviates because our model assumption does not hold if the injected traffic is close to the network capacity as discussed previously. However, for $12\,\mathrm{Mbit/s}$, the simulation results show a significant increase in delay compared to the analytical results beyond the network size of 176. This is due to the limited data rate to support the offered load resulting in an exponential increase of retransmissions (refer Fig. 5b).

VI. CONCLUSION

In this paper, we presented an analytical model for the IEEE 802.11 DCF that serves as a general tool for evaluating the performance of single-hop WGNs in seismic applications. In addition, the model also serves as a tool for quick parameter studies (like data rate, packet size, optimal number of geophones in a subnetwork e.t.c.), for realizing our

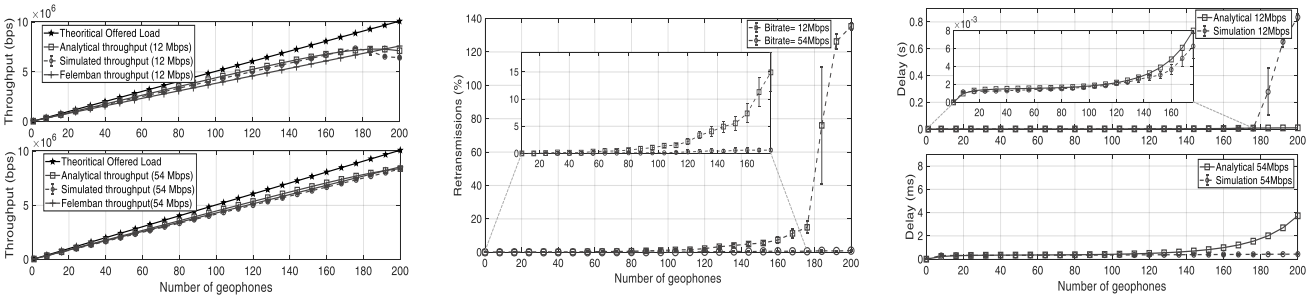

(a) Analytical and simulated throughput vs number of nodes.

(b) Packet retransmission ratio captured from the simulation vs number of nodes.

(c) Analytical and simulated MAC delay vs number of nodes.

Fig. 5: Model validation

proposed architecture for WSDA network presented in [16]. An extension of the classical Markov model that describes the DCF behavior which accounts for the packet drop probability, backoff counter decrementing probability, unsaturated traffic condition, and average duration a node spends before decrementing its counter during the backoff process was presented. The model performance was validated using simulations for varying number of geophone nodes and data rates. Results show that, with higher data rates, more number of geophones can be accommodated within a subnetwork in the architecture proposed in [16]. However, with lower data rates, beyond a certain number of geophones in the network, the assumption of binary queue does not hold due to the increased offered traffic which approaches the maximum capacity the network can handle, resulting in increased retransmissions. This effect could be a problem in multi-hop WGNs since packets need to traverse multiple hops before reaching its destination. Thus, a subnetwork size with the highest throughput performance, low delay, and significantly less number of retransmissions is optimal, especially when considering multi-hop WSDA network scenarios. Future work will be directed towards extending the model presented to evaluate performance of multi-hop WSDA networks, which will depend on the routing strategy employed at the upper layer.

ACKNOWLEDGMENT

This work is supported by Deutscher Akademischer Austauschdienst (DAAD) under the Nigerian-German Postgraduate Training Programme (57401043), in collaboration with the Nigerian Petroleum Technology Development Fund (PTDF). Furthermore, we thank Leonard Fisser for his input and valuable discussions.

REFERENCES

[1] G. Vermeer, "3-D Seismic Survey Design," Society of Exploration Geophysicists, 2002.

[2] "IEEE Standard for Information Technology–Telecommunications and Information Exchange between Systems - Local and Metropolitan Area Networks–Specific Requirements - Part 11: Wireless LAN Medium Access Control (MAC) and Physical Layer (PHY) Specifications," IEEE Std 802.11-2020 (Revision of IEEE Std 802.11-2016), Feb. 2021.

[3] G. Bianchi, "Performance analysis of the IEEE 802.11 distributed coordination function," IEEE Journal on Selected Areas in Communications, vol. 18, no. 3, pp. 535–547, Mar. 2000.

[4] Z. Hadzi-Velkov and B. Spasenovski, "Saturation throughput - delay analysis of IEEE 802.11 DCF in fading channel," in IEEE International Conference on Communications, May 2003, vol. 1, pp. 121–126.

[5] Y. Lin and V. W. S. Wong, "WSN01-1: Frame Aggregation and Optimal Frame Size Adaptation for IEEE 802.11n WLANs," in IEEE Globecom 2006, Nov. 2006, pp. 1–6.

[6] Z. Chang et al., "Performance Analysis of IEEE 802.11ac DCF with Hidden Nodes," in 2012 IEEE 75th Vehicular Technology Conference (VTC Spring), May 2012, pp. 1–5.

[7] S. M. Mirrezaei, K. Faez, and A. Ghasemi, "Performance Analysis of Network Coding Based Two-Way Relay Wireless Networks Deploying IEEE 802.11," Wireless Pers Comm, vol.76, no.1, pp. 41–76, May 2014.

[8] D. Malone, K. Duffy, and D. Leith, "Modeling the 802.11 Distributed Coordination Function in Nonsaturated Heterogeneous Conditions," IEEE/ACM Transactions on Networking, vol. 15, no. 1, Feb. 2007.

[9] H. Zhai, Y. Kwon, and Y. Fang, "Performance analysis of IEEE 802.11 MAC protocols in wireless LANs," Wireless Communications and Mobile Computing, vol. 4, no. 8, pp. 917–931, 2004.

[10] O. Tickoo and B. Sikdar, "Modeling Queueing and Channel Access Delay in Unsaturated IEEE 802.11 Random Access MAC Based Wireless Networks," IEEE/ACM Transactions on Networking, vol. 16, no. 4, pp. 878–891, Aug. 2008.

[11] Y. Xiao, "Performance analysis of priority schemes for IEEE 802.11 and IEEE 802.11e wireless LANs," IEEE Transactions on Wireless Communications, vol. 4, no. 4, pp. 1506–1515, Jul. 2005.

[12] Y. Barowski, S. Biaz, and P. Agrawal, "Towards the performance analysis of IEEE 802.11 in multi-hop ad-hoc networks," in IEEE Wireless Communications and Networking Conference, vol. 1, 2005.

[13] P. Chatzimisios, A. C. Boucouvalas, and V. Vitsas, "IEEE 802.11 packet delay-a finite retry limit analysis," in GLOBECOM '03. IEEE Global Telecommunications Conference (IEEE Cat. No.03CH37489), Dec. 2003, vol. 2, pp. 950-954.

[14] A. Alshanyour and A. Agarwal, "Three-Dimensional Markov Chain Model for Performance Analysis of the IEEE 802.11 Distributed Coordination Function," in GLOBECOM 2009, Nov. 2009.

[15] F. Daneshgaran, M. Laddomada, F. Mesiti, and M. Mondin, "Unsaturated Throughput Analysis of IEEE 802.11 in Presence of Non Ideal Transmission Channel and Capture Effects," IEEE Transactions on Wireless Communications, vol. 7, no. 4, pp. 1276–1286, Apr. 2008.

[16] A. Makama, K. Kuladinithi, and A. Timm-Giel, "Wireless Geophone Networks for Land Seismic Data Acquisition: A Survey, Tutorial and Performance Evaluation," Sensors, vol. 21, Art. no. 15, Jan. 2021.

[17] A. Makama, K. Kuladinithi, M. E. A. Ahmed, and A. Timm-Giel, "Evaluation of Multi-hop Ad-hoc Routing Protocols in Wireless Seismic Data Acquisition," Electronic Communications of the EASST, vol. 80, Sep. 2021.

[18] E. Felemban and E. Ekici, "Single Hop IEEE 802.11 DCF Analysis Revisited: Accurate Modeling of Channel Access Delay and Throughput for Saturated and Unsaturated Traffic Cases," IEEE Transactions on Wireless Communications, vol. 10, no. 10, pp. 3256–3266, Oct. 2011.

[19] "OMNeT++ Discrete Event Simulator." https://omnetpp.org/ (accessed Apr. 04, 2022).